THE DYNAMICS OF VORTEX FILAMENTS WITH CORNERS

LUIS VEGA

1. Introduction

In these pages I shall sketch some recent work about the evolution of vortex filaments that follow the geometric law of the binormal: a point of the filament moves in the direction of the binormal with a speed that is proportional to the curvature. First I shall consider the case of a curve (filament) that is regular except at a point where it has a corner (joint work with V. Banica). Then, I shall look at the case of a regular polygon (joint work with F. de la Hoz).

Therefore at some point we will have to answer the simple question: **What is the velocity of the corner?**

The motivation of this geometric flow comes from fluid dynamics. In particular the well known smoke rings as those seen in figure 1. What we see in the picture are "vortex tubes" that propagate in a self-similar way. These vortex tubes have two distinguished parts. A first one which looks very much as a horseshoe, and a second one with a helicoidal shape. In figure 2 we see some vortices above an inclined triangular wing. Again self-similarity is evident together with the pair of symmetrical helices winding around two lines.

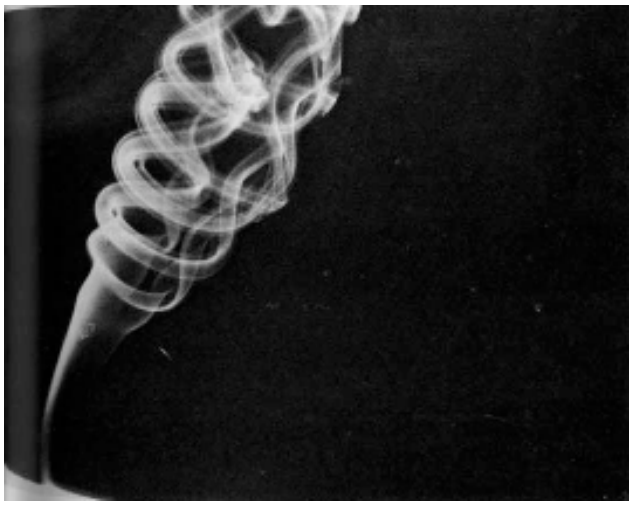

Figure 1.

Partially supported by the grants MTM2011-24054, UFI11/52 and IT-305-07.

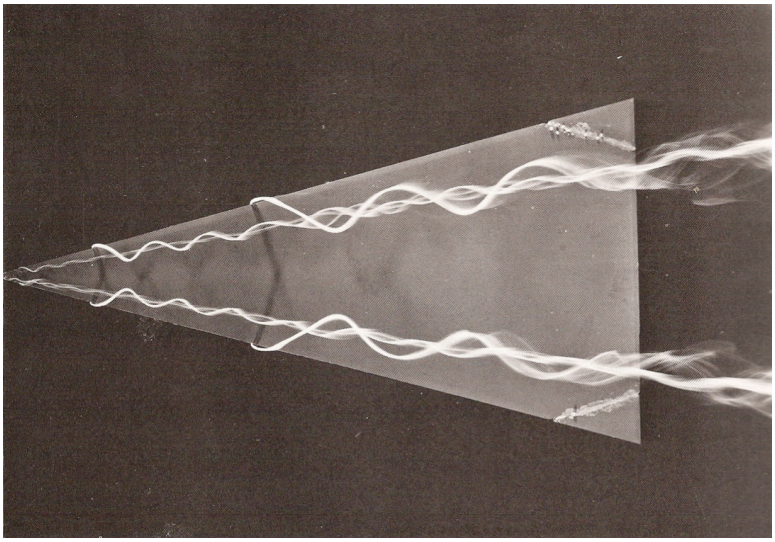

FIGURE 2.

A first simplification to describe mathematically what we see in the above two figures is to forget viscosity effects and consider that the fluids satisfy Euler equations. Therefore we have to give $\mathbf{u}$ the velocity field or as an alternative the vorticity

$$\omega = \operatorname{curl} \mathbf{u} = \nabla \wedge \mathbf{u}.$$

In our case the vorticity is a singular vector measure that has the support on a curve $\mathbf{X}$ in $\mathbb{R}^3$

$$\omega = \Gamma \mathbf{T} ds \qquad \mathbf{T} = \mathbf{X}_s.$$

Above Γ is the circulation that is a constant. Together with the inviscid condition

$$div\, \mathbf{u} = 0,$$

we can use the so-called Biot-Savart law

$$\mathbf{u}(P) = \frac{\Gamma}{4\pi} \int_{-\infty}^{\infty} \frac{\mathbf{X}(s) - \mathbf{P}}{|\mathbf{X}(s) - \mathbf{P}|^3} \wedge \mathbf{T}(s) ds, \tag{1}$$

to obtain the velocity at any point $\mathbf{P}$ that is not in the curve $\mathbf{X}(s,t)$. Particular examples are the straight lines and vortex rings. Straight lines do not move and are mathematical idealizations of bathtub vortices. Vortex rings do not change their shape and move perpendicularly to the plane where they are contained and in a direction that is determined by the sign of Γ. We encourage the reader to see the movie `http://news.uchicago.edu/multimedia/vortex-tied-knots` where the evolution of different vortex filaments can be seen and in particular the case of one ring. Finally particular solutions of Euler equations with $\mathbf{X}$ with a helicoidal shape are known since the work of Hardin [14].

In order to compute the velocity of the curve we should be able to compute (1) for a point of the curve, say $\mathbf{X}(s_0, t)$. A simple look at the Biot-Savart integral tells us that this is not an easy task unless some simplifications are done. The simplest one is

to consider that just local effects are relevant and to make a Taylor expansion around $s = s_0$ to capture them. The first term is determined by the tangent at that point. If this term is the only one considered it is like changing the curve for the tangent line at that point and therefore the overall contribution to the velocity field is zero. As can be expected the next relevant term has a singularity that depends logarithmically with the distance of P to $\mathbf{X}(s_0, t)$. The usual procedure, that goes back to Da Rios in 1906 [7] (see also [16] for the details and the limitations of this approach) is to renormalize the time variable to avoid this singularity. After this renormalization and making all the relevant constants equal to unity we are lead to the equation

$$\mathbf{X}_t = \mathbf{X}_s \wedge \mathbf{X}_{ss}. \tag{2}$$

Calling

$$\begin{aligned} &c = c(s,t) && \text{curvature} \\ &\tau = \tau(s,t) && \text{torsion} \\ &\mathbf{n} = \mathbf{n}(s,t) \in \mathbb{R}^3 && \\ &\mathbf{b} = \mathbf{b}(s,t) && \text{binormal,} \end{aligned}$$

we get from Frenet equations

$$\begin{array}{rcrcl} \mathbf{T}_s & = & & c\mathbf{n} & \\ \mathbf{n}_s & = & -c\mathbf{T} & & +\tau\mathbf{b} \\ \mathbf{b}_s & = & & -\tau\mathbf{n} & \end{array} \tag{3}$$

that (2) can be rewritten as

$$\mathbf{X}_t = c\mathbf{b}. \tag{4}$$

Particular examples are the straight line, the circle, that are obvious, and the helix. The helix is easily obtained solving the equation that the tangent vector $\mathbf{T}$ satisfies. In fact, differentiating with respect to the spatial variable in (2) we get

$$\mathbf{T}_t = \mathbf{T} \wedge \mathbf{T}_{ss}. \tag{5}$$

If we look for traveling wave solutions $\mathbf{T}(s,t) = \mathbf{R}(s - bt)$ we get from (5)

$$-a\mathbf{R}' = \mathbf{R} \wedge \mathbf{R}''.$$

From (3) we obtain

$$-b\, c\mathbf{n} = \mathbf{R} \wedge \left(c'\mathbf{n} - c^2\mathbf{R} + c\tau\mathbf{b}\right).$$

As a consequence $c' = 0$. Hence $c = a$ and $\tau = b$, and therefore we have a helix.

Several remarks about (2) are in order

Remark 1.

- $|T|^2 =$ *constant. This follows immediately form* (5)*;*
- *Equation* (2) *is time reversible: If* $\mathbf{X}$ *is a solution, so is* $\widetilde{\mathbf{X}}(s,t) = \mathbf{X}(-s,-t)$*. In other words, a reorientation of the curves is equivalent to change the direction of time,*
- *The equation is rotation invariant.*

2. Self-similar Solutions

It seems very natural after looking at the figures 1 and 2 to look for self-similar solutions of (1). That is to say, solutions $\mathbf{X}$ that can be written as

$$\mathbf{X}(s,t) = \sqrt{t}\mathbf{G}\left(s/\sqrt{t}\right) \tag{6}$$

for some $\mathbf{G}$. If we call $\mathbf{G}_s = \mathbf{R}$ and take $\mathbf{T}(s,t) = \mathbf{R}\left(s/\sqrt{t}\right)$ we get from (3) that

$$-\frac{s}{2}\mathbf{R}' = \mathbf{R} \wedge \mathbf{R}''.$$

Using again Frenet equations (2) we obtain this time

$$-\frac{s}{2}c\mathbf{n} = \mathbf{R} \wedge \left(c'\mathbf{n} - c^2\mathbf{R} + c\tau\mathbf{b}\right).$$

Hence $c' = 0$ so that $c = a$ and $\tau = s/2$ (see [6]). In figure 3 we see a self-similar solution (6) for some choice of $\mathbf{G}$.

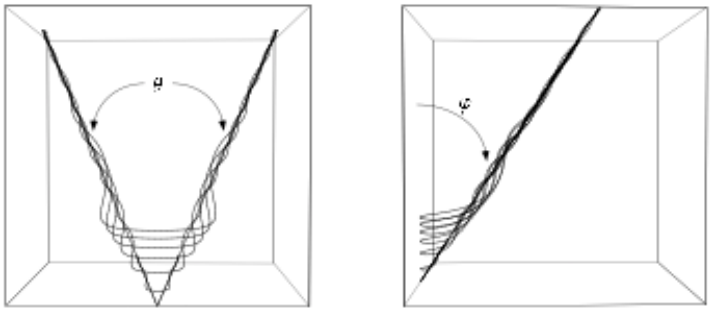

Figure 3.

The self-similar solutions and its characterizations were studied in [12]. In particular a characterization of them in terms of the parameter a is obtained. It is also proved that at time zero they have the shape of two half lines joined together at $s = 0$ with an angle θ. The curve $\mathbf{G}$ tends asymptotically to these two lines. Also precise expressions of θ and the angle φ in terms of a are given. Finally observe that the right hand side of figure 2 indicates that the corner moves in a very precise way: the speed is $a/\sqrt{t}$ and the direction is determined by the angle φ. In figure 4 we compare the dynamics of self-similar solutions with the vortices above an inclined triangular wing given in figure 2. The similitude at the qualitative level is quite appealing.

3. Schrödinger Equation

An important step in the understanding of (1) was given by Hasimoto in [13]. He introduces the transformation

$$\psi(s,t) = c(s,t)e^{i\int_0^s \tau(s',t)ds'}. \tag{7}$$

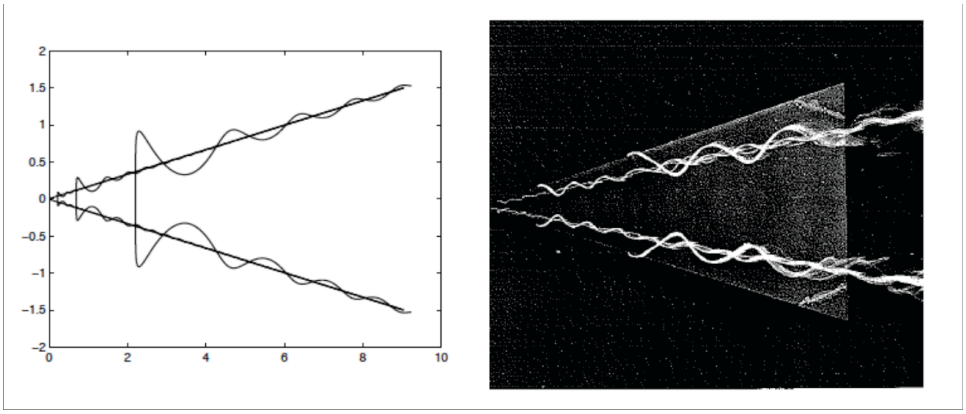

FIGURE 4.

After some calculations he proves that if $\mathbf{X}$ solves (1) then ψ solves

$$\partial_t \psi(s,t) = i\left(\partial_s^2 \psi + \frac{1}{2}(|\psi|^2 + A(t))\psi\right) \tag{8}$$

for some $A(t) \in \mathbb{R}$.

Therefore it is straightforward that for regular solutions of (8)

$$\int_{-\infty}^{\infty} |\psi(s,t)|^2 ds = \int_{-\infty}^{\infty} |\psi(s,0)|^2 ds = \int_{-\infty}^{\infty} c^2(s,0) ds. \tag{9}$$

In fact to solve (8) under the condition that (9) is finite is nowadays quite standard. However in our case:

$$\psi(s,t) = \frac{a}{\sqrt{t}} e^{i\frac{s^2}{4t}} \qquad , \qquad \int_{-\infty}^{\infty} |\psi|^2 ds = +\infty.$$

Our next step is to extend the self-similar solutions for negative times. Formally this can be easily done using remark 1. As we said to change the direction of time is enough to change the orientation of the curve at time zero. In our case this can be done using a rotation ρ that interchanges the two lines that generate the initial curve. Then, it is enough to apply this rotation ρ to the curve $\sqrt{t}\mathbf{G}(s/\sqrt{t})$ as done in figure 5. We have the following result.

Theorem 3.1. *The self-similar solutions exhibited in figure 5 are stable. In particular, the creation/annihilation of a corner is a stable procedure.*

The proof of this result is a consequence of several papers done in collaboration with V. Banica (see [1], [2], [3], and [4]). We also refer the reader to [4] for a precise statement of the above theorem. The proof follows the following steps:

- A pseudo-conformal transformation of ψ is done. This implies to change the variable t into $1/t$ so that the initial value problem for (9) becomes a scattering problem. Therefore the existence of the wave operator and its asymptotic completeness have to be settled.

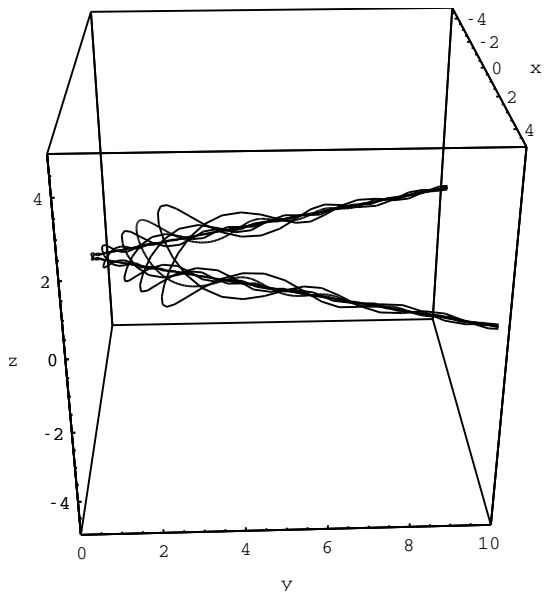

FIGURE 5.

- For dealing with the scattering problem the right space of functions has to be found.
- Extra difficulties come from the fact that the non-linear potential is a long range potential. This has an important consequence: cubic NLS equation (9) with the Dirac–delta as initial condition is ill–posed. Observe that the Dirac-delta is the initial condition of (9) (with $A(t) = \frac{a^2}{t}$) that isassociated to a self-similar solution.
- As a consequence, for describing the formation of a corner at time $t = 0$ one can not work just with (9). It is also necessary to work with (1) and (3). The recipe to go beyond $t = 0$ is to use a blow–up argument to "capture" the appropriate selfsimilar solution.
- For the last step the characterization of the self-similar solutions obtained in [12] plays a fundamental role.

4. A Regular Polygon

Our next step is to consider solutions of (1) that at time $t = 0$ are given by a regular polygon. In terms of the Hasimoto function (7) a planar regular polygon with M sides is described as

$$\psi(s,0) = \frac{2\pi}{M} \sum_{k=-\infty}^{\infty} \delta\left(s - \frac{2\pi k}{M}\right). \tag{10}$$

Let us recall the so-called galilean transformations: if $\psi(s,t)$ is a solution of (9) then

$$\tilde{\psi}(s,t) \equiv e^{iks - ik^2 t}\psi(s - 2kt, t), \quad \forall\, k, t \in \mathbb{R},$$

is also solution. Observe that for $\psi(s,0)$ as in (10) then

$$e^{2\pi ijMs}\psi(s,0) = \psi(s,0) \quad \forall\, j \in \mathbb{Z}.$$

Therefore if there were uniqueness for the initial value problem (9) with initial condition (10) then

$$\tilde{\psi}_k = \psi \quad \forall\, k \in \mathbb{Z}.$$

This has very strong consequences because if we define

$$\widehat{\psi}(j,t) = \frac{M}{2\pi}\int_0^{2\pi/M} e^{-iMjs}\psi(s,t)ds$$

then

$$\begin{aligned}
\widehat{\psi}(j,t) &= \frac{M}{2\pi}\int_0^{2\pi/M} e^{-iMjs}\psi(s,t)ds \\
&= \frac{M}{2\pi}\int_0^{2\pi/M} e^{-iMjs}\left[e^{iMks-i(Mk)^2t}\psi(s-2Mkt,t)\right]ds \\
&= \frac{Me^{-i(Mk)^2t}}{2\pi}\int_0^{2\pi/M} e^{-iM(j-k)s}\psi(s-2Mkt,t)ds \\
&= \frac{Me^{-i(Mk)^2t}}{2\pi}\int_0^{2\pi/M} e^{-iM(j-k)(s+2Mkt)}\psi(s,t)ds \\
&= \frac{Me^{-i(Mk)^2t-iM(j-k)(2Mkt)}}{2\pi}\int_0^{2\pi/M} e^{-iM(j-k)s}\psi(s,t)ds \\
&= e^{-i(Mk)^2t-iM(j-k)(2Mkt)}\widehat{\psi}(j-k,t).
\end{aligned}$$

Therefore

$$\widehat{\psi}(j,t) = e^{-i(Mj)^2t}\widehat{\psi}(0,t) \qquad \text{for all } j.$$

Now for "rational times"

$$t_{pq} = 2\pi p/(M^2q)$$

we get

$$\begin{aligned}
\psi(s,t_{pq}) &= \widehat{\psi}(0,t_{pq})\sum_{k=-\infty}^{\infty} e^{-i(Mk)^2 2\pi p/(M^2q)+iMks} \\
&= \widehat{\psi}(0,t_{pq})\sum_{k=-\infty}^{\infty} e^{-2\pi i(p/q)k^2+iMks} \\
&= \widehat{\psi}(0,t_{pq})\sum_{l=0}^{q-1}\sum_{k=-\infty}^{\infty} e^{-2\pi i(p/q)(qk+l)^2+iM(qk+l)s} \\
&= \widehat{\psi}(0,t_{pq})\sum_{l=0}^{q-1} e^{-2\pi i(p/q)l^2+iMls}\sum_{k=-\infty}^{\infty} e^{iMqks}.
\end{aligned}$$

This is the so-called Talbot effect – see [5] and [8]. Observe that in our case this Talbot effect is understood geometrically by observing that at time t_{pq} a new polygon with Mq

sides is generated. This polygon is determined by the generalized quadratic Gauss sums that are defined by

$$\sum_{l=0}^{|c|-1} e^{2\pi i(al^2+bl)/c},$$

for given integers a, b, c, with $c \neq 0$.

It is well known that

$$G(-p,m,q) = \begin{cases} \sqrt{q}e^{i\theta m}, & \text{if } q \text{ is odd,} \\ \sqrt{2q}e^{i\theta m}, & \text{if } q \text{ is even and } q/2 \equiv m \mod 2, \\ 0, & \text{if } q \text{ is even and } q/2 \not\equiv m \mod 2, \end{cases} \tag{11}$$

for a certain angle θ_m that depends on m, p, and q.

Gathering all the information we get

$$\psi(s,t_{pq}) = \begin{cases} \displaystyle\sum_{m=0}^{q-1} (\alpha_m + i\beta_m)\,\delta\left(s - \frac{2\pi m}{Mq}\right), & \text{if } q \text{ is odd,} \\ \displaystyle\sum_{m=0}^{q/2-1} (\alpha_{2m+1} + i\beta_{2m+1})\,\delta\left(s - \frac{4\pi m + 2\pi}{Mq}\right), & \text{if } q/2 \text{ is odd,} \\ \displaystyle\sum_{m=0}^{q/2-1} (\alpha_{2m} + i\beta_{2m})\,\delta\left(s - \frac{4\pi m}{Mq}\right), & \text{if } q/2 \text{ is even,} \end{cases}$$

where

$$|\alpha_m + i\beta_m| = \begin{cases} \dfrac{2\pi}{M\sqrt{q}}\widehat{\psi}(0,t_{pq}), & \text{if } q \text{ is odd,} \\ \dfrac{2\pi}{M\sqrt{\frac{q}{2}}}\widehat{\psi}(0,t_{pq}), & \text{if } q \text{ is even and } q/2 \equiv m \mod 2, \\ 0, & \text{if } q \text{ is even and } q/2 \not\equiv m \mod 2, \end{cases}$$

so we conclude that the angle ρ between two adjacent sides is constant. Furthermore, writing

$$\alpha_m + i\beta_m = \rho e^{i\theta_m}$$

we see that the structure of the polygon is given by the angles θ_m.

Bearing in mind that ψ is given as a sum of δ-functions it is more appropriate to use the so-called parallel frame than the Frenet frame,

$$\begin{pmatrix} \mathbf{T} \\ \mathbf{e}_1 \\ \mathbf{e}_2 \end{pmatrix}_s = \begin{pmatrix} 0 & \alpha & \beta \\ -\alpha & 0 & 0 \\ -\beta & 0 & 0 \end{pmatrix} \cdot \begin{pmatrix} \mathbf{T} \\ \mathbf{e}_1 \\ \mathbf{e}_2 \end{pmatrix}.$$

Hence we have to solve systems of the type

$$\begin{pmatrix} \mathbf{T} \\ \mathbf{e}_1 \\ \mathbf{e}_2 \end{pmatrix}_s = \begin{pmatrix} 0 & a\delta & b\delta \\ -a\delta & 0 & 0 \\ -b\delta & 0 & 0 \end{pmatrix} \cdot \begin{pmatrix} \mathbf{T} \\ \mathbf{e}_1 \\ \mathbf{e}_2 \end{pmatrix}.$$

It is immediate to obtain

$$\begin{aligned} \begin{pmatrix} u_1(0^+) \\ u_2(0^+) \\ u_3(0^+) \end{pmatrix} &= \exp\left[\begin{pmatrix} 0 & a & b \\ -a & 0 & 0 \\ -b & 0 & 0 \end{pmatrix} \int_{0^-}^{0^+} \delta(s')ds' \right] \cdot \begin{pmatrix} u_1(0^-) \\ u_2(0^-) \\ u_3(0^-) \end{pmatrix} \\ &= \exp\left[\begin{pmatrix} 0 & a & b \\ -a & 0 & 0 \\ -b & 0 & 0 \end{pmatrix} \right] \cdot \begin{pmatrix} u_1(0^-) \\ u_2(0^-) \\ u_3(0^-) \end{pmatrix} \end{aligned}$$

We still have to determined $\widehat{\psi}(0,t)$. We will do it by imposing that the polygon has to be closed. Observe that to compute the k-side we have to write

$$\begin{pmatrix} \mathbf{T}\left(\frac{2\pi k^+}{Mq}\right)^T \\ \hline \mathbf{e}_1\left(\frac{2\pi k^+}{Mq}\right)^T \\ \hline \mathbf{e}_2\left(\frac{2\pi k^+}{Mq}\right)^T \end{pmatrix} = \mathbf{M}_k \cdot \mathbf{M}_{k-1} \cdot \ldots \cdot \mathbf{M}_1 \cdot \mathbf{M}_0 \cdot \begin{pmatrix} \mathbf{T}\,(0^-)^T \\ \hline \mathbf{e}_1\,(0^-)^T \\ \hline \mathbf{e}_2\,(0^-)^T \end{pmatrix}.$$

Hence, for the polygon to be closed it is necessary that

$$\mathbf{M}_{Mq-1} \cdot \mathbf{M}_{Mq-2} \cdot \ldots \cdot \mathbf{M}_1 \cdot \mathbf{M}_0 \equiv \mathrm{I}.$$

Let us define:

$$\mathbf{M} = \mathbf{M}_{q-1} \cdot \mathbf{M}_{q-2} \cdot \ldots \cdot \mathbf{M}_1 \cdot \mathbf{M}_0.$$

Therefore, $\mathbf{M}$ is an M–th root of the identity matrix and also a rotation matrix that induces a rotation of $2\pi/M$ degrees around a certain rotation axis. Hence

$$\begin{aligned} \mathrm{Tr}\,(\mathbf{M}) &= 1 + 2\cos\left(\frac{2\pi}{M}\right), \\ \sigma(\mathbf{M}) &= \left\{1, e^{2\pi i/M}, e^{-2\pi i/M}\right\}. \end{aligned}$$

From this fact and some strong numerical evidence we conjecture that

$$\cos(\rho) = \begin{cases} 2\cos^{2/q}(\pi/M) - 1, & \text{if } q \text{ is odd}, \\ 2\cos^{4/q}(\pi/M) - 1, & \text{if } q \text{ is even}. \end{cases}$$

As a consequence of the previous arguments we have all the necessary information to compute $\mathbf{T}$ at $t = t_{pq}$, except that we need the trajectory of one point. This is obtained using the symmetries of the $M-$polygon as it is explained in [15].

In figure 6 we compare the numerical solution with the theoretical one, the construction of which we have just sketched. We see that there is a remarkable agreement between the two.

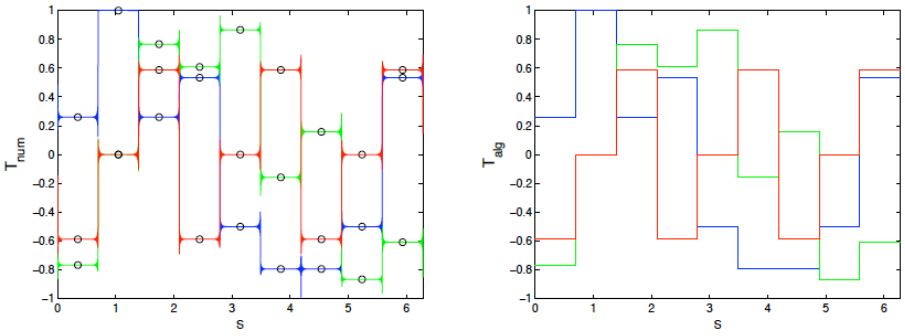

FIGURE 6. $\mathbf{T}_{num}$ versus $\mathbf{T}_{alg}$, for $M = 3$, at $T_{1,3} = \dfrac{2\pi}{27}$. T_1 appears in blue, T_2 in green, T_3 in red. In $\mathbf{T}_{num}$, the Gibbs phenomenon is clearly visible. The black circles denote the points chosen for the comparisons.

It is interesting to observe the trajectory of one of the corners as for example $\mathbf{X}(0,t)$. Using again the symmetries of the M-polygon is easy to see that this trajectory falls in a plane. In figures 7 and 8 we can see the particular cases of the equilateral triangle and the square.

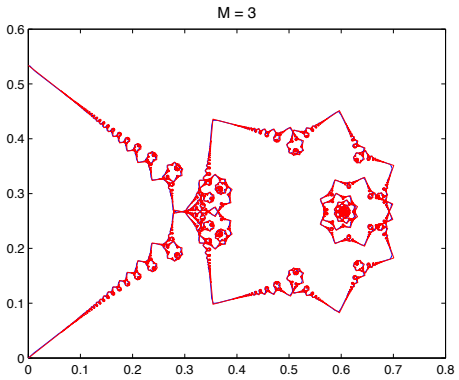

FIGURE 7.

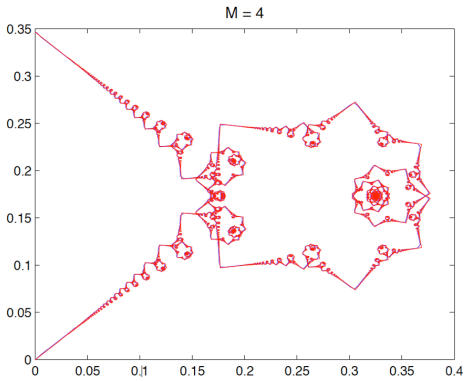

FIGURE 8.

These pictures are quite reminiscent of the so-called Riemann's non-differentiable function

$$\phi(t) = \sum_{k\neq 0} \frac{e^{-2\pi i t k^2}}{k^2}. \tag{12}$$

Observe that $\phi(1) = \phi(0)$. Renormalizing $\mathbf{X}(0,t)$ accordingly we see in figures 9, 10 and 11 that at the qualitative level there is a big similitude between them. This similitude becomes stronger the bigger the M. This is numerically proved in [15]. In [9] it is proved that the graph given by ϕ in (12) is a multi-fractal that satisfies the so-called Frisch-Parisi conjecture –see [10] and [11].

I want to finish with a few remarks about the behavior of real fluids. The results in [15], some of which have been sketched in this note, suggest that at half of a period the starting regular polygon with M sides becomes the same polygon but with the axis switched with an angle equal to π/M. Observe that at those times, and due to the fact that $q = 2$, the Gauss sum is zero for half of the cases in (11), so that the polygon has M sides instead of $2M$. Then, the axis switching phenomena follows from the analysis of which are the precise values of m in (11) that make the Gauss sum trivial. It turns out that this phenomena has been observed in real fluids, in particular for non-circular jets, and it is well documented. We refer the reader to [15] for the appropriate references. In figure 12 the reader will find some pictures of a domestic experiment. A smoke cannon made with a cardboard box that has a hole with the shape of an equilateral triangle is used. After introducing some smoke through the hole the box is suddenly hit at the back. A camera in front of the box is located. The first three pictures clearly illustrate the flip-flop of the triangle as a consequence of the switching of the axis by a $\pi/3$-angle. Or course the corners are smoothed out due to the effects of the viscosity. Our analysis also implies that skew polygons with six sides should appear as a consequence of the Talbot effect mentioned above. The last picture in figure 12 is not conclusive and further evidence in this direction is needed.

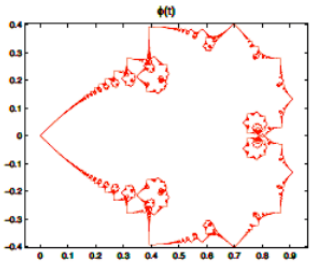

FIGURE 9.

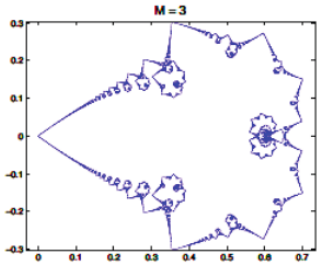

FIGURE 10.

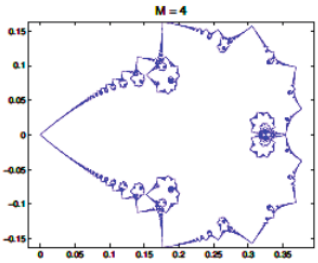

FIGURE 11.

REFERENCES

[1] V. Banica and L. Vega, *On the stability of a singular vortex dynamics*, Comm. Math. Phys. **286** (2009), 593–627.

[2] V. Banica and L. Vega, *Scattering for 1D cubic NLS and singular vortex dynamics*, J. Eur. Math. Soc. **14** (2012), 209–253.

[3] V. Banica and L. Vega, *Stability of the self-similar dynamics of a vortex filament*, ArXiv:1202.1106.

[4] V. Banica and L. Vega, *The initial value problem for the binormal flow with rough data* arXiv:1304.0996.

[5] M. V. Berry and J. Goldberg, *Renormalisation of curlicues* Nonlinearity, **1** (1) (1988), 1–26.

FIGURE 12.

[6] T. F. Buttke, *A numerical study of superfluid turbulence in the Self Induction Approximation*, J. of Compt. Physics **76** (1988), 301–326

[7] L. S. Da Rios, *On the motion of an unbounded fluid with a vortex filament of any shape*, Rend. Circ. Mat. Palermo **22** (1906), 117.

[8] M. B. Erdogan, N. Tzirakis, *Talbot effect for the cubic nonlinear Schrödinger equation on the torus*, arXiv:1303.3604.

[9] S. Jaffard, *The spectrum of singularities of Riemann's function*, Rev. Mat. Iberoamericana, **12**(1996) (2):441–460,

[10] U. Frisch and G. Parisi, *Fully developed turbulence and intermittency*, Proc. Int. Sch. Phys. "Enrico Fermi", North-Holland, Amsterdam, 1985.

[11] U. Frisch. Turbulence. The Legacy of A. N. Kolmogorov. Cambridge University Press, 1995.

[12] S. Gutiérrez, J. Rivas and L. Vega, *Formation of singularities and self-similar vortex motion under the localized induction approximation*, Comm. Part. Diff. Eq. **28** (2003), 927–968.

[13] H. Hasimoto, *A soliton in a vortex filament,* J. Fluid Mech. **51** (1972), 477–485.

[14] Hardin J. C., *The velocity field induced by a helical vortex filament,* Phys. Fluids **25** 1982, 1949–1952

[15] F. de la Hoz and L. Vega, *Vortex Filament Equation for a Regular Polygon* arXiv:1304.5521

[16] Saffman, P. G. *Vortex dynamics,* Cambridge Monographs on Mechanics and Applied Mathematics. Cambridge University Press, New York, 1992.

(L. Vega) DEPARTAMENTO DE MATEMATICAS, UNIVERSIDAD DEL PAIS VASCO & BCAM, BILBAO, SPAIN

E-mail address: luis.vega@ehu.es, lvega@bcamath.org